

Nonequilibrium electron transport in wide miniband GaAs/Al_xGa_{1-x}As superlattices at room temperature

S. Madhavi,* M. Abe, Y. Shimada, and K. Hirakawa*[†]

Institute of Industrial Science, University of Tokyo, 4-6-1 Komaba, Meguro-ku, Tokyo 153-8505, Japan

(Received 28 February 2002; published 7 May 2002)

Nonequilibrium electron transport in a GaAs/Al_{0.3}Ga_{0.7}As superlattice with a miniband width of 100 meV has been investigated by time-domain terahertz spectroscopy. When the superlattice is pumped at the bottom of the miniband, the transient electron velocity is found to exhibit acceleration-deceleration characteristics unique to miniband dispersion. The time taken to reach the steady-state velocity was determined to be of the order of 1–2 ps. When pumped at the top of the miniband, no phase reversal in the transient velocity was observed, indicating the importance of the density of photoexcited states by femtosecond laser pulses.

DOI: 10.1103/PhysRevB.65.193308

PACS number(s): 78.47.+p, 73.21.Cd, 72.20.Ht

The sophistication of crystal growth technologies over the last few decades has helped realize the ideas of Esaki and Tsu¹ and has made it possible to tailor the superlattice (SL) parameters with great accuracy. This was followed by many experiments to study the electronic properties of SL's and also led to the experimental observation of the theoretically predicted Wannier-Stark quantization of the miniband in the presence of large electric fields.^{2–4} More recently, femtosecond-time-resolved optical studies were carried out successfully to observe Bloch oscillations at low and room temperatures,^{5–16} which settled the ongoing arguments regarding their existence.

Along with these optical properties, transport properties of doped SL's have also been extensively studied^{17–21} and, in particular, wide miniband SL structures have recently attracted a lot of interest mainly due to their potential applications to high-frequency oscillators. High-frequency transit-time current oscillations with frequencies up to 100 GHz have been reported recently in doped wide miniband SL structures.²² These oscillations were understood to be due to the formation of traveling dipole domains, which originate from the negative differential velocities (NDV's) of electrons intrinsic to miniband dispersion. The frequency of such traveling domain oscillations is higher for wider miniband widths owing to larger domain velocities.²³ However, a complete understanding of the dynamical transport properties of carriers in SL's is still lacking, which is very essential for designing high-frequency SL oscillators.

A direct measurement of electron velocity in perpendicular transport will present a clear picture of the Bloch transport characteristics of SL's and aid in the complete understanding of their electrical properties. The purpose of this paper is to bridge the optical and transport properties of SL's and obtain deeper insight into the high-frequency properties of SL's. With the advancement in time-domain terahertz (THz) spectroscopy, it has become possible to study ultrafast transport phenomena in condensed matter, which were hitherto beyond the scope of experimental observation. Recently, this technique was applied to measure directly the velocity overshoot phenomenon in bulk compound semiconductors.²⁴

In this work, we have employed this technique to measure the transient complex current change through a GaAs/Al_{0.3}Ga_{0.7}As SL and determined the transient velocity

response of electrons in a wide miniband SL. The transient velocity of electrons exhibits a peak followed by a decrease before reaching a steady state, characteristics of miniband transport. The time taken to reach steady-state velocity was determined to be of the order of 1–2 ps. We have also studied the pump photon energy dependence of the transient velocity response and noticed an importance of the preparation of initial wave packets by femtosecond laser pulses.

The sample used in the present work was an undoped GaAs/Al_{0.3}Ga_{0.7}As SL with 73 periods of 6.3-nm-thick GaAs wells and 0.7-nm-thick Al_{0.3}Ga_{0.7}As barrier layers (periodicity d of 7 nm) grown on an n^+ -GaAs (100) substrate by molecular beam epitaxy. The width of the first electron miniband, Δ , in this sample was designed to be 100 meV, which is much larger than the longitudinal optical phonon energy in GaAs and confirmed by weak-excitation photocurrent measurements.²⁵ We fabricated a m - i - n (metal-intrinsic- n -type) diode by depositing a semitransparent 4-nm-thick NiCr layer on the sample surface over an area of approximately 2.5 mm². An Ohmic contact was fabricated on the back surface by depositing and annealing AuGeNi alloy. A dc bias field F was applied between these two electrodes. In order to create carriers in the miniband, the sample surface was illuminated with femtosecond laser pulses from a tunable Ti:Al₂O₃ laser operated at a repetition frequency of 76 MHz. The spectral width of the laser pulses was 15 nm. The photoexcited carrier density was maintained below $1 \times 10^{15} \text{ cm}^{-3}$ in order to avoid field screening by photoexcited carriers.

The photoexcited carriers in the undoped SL are accelerated by the dc electric field, and the THz electromagnetic wave, whose electric field component E_{THz} is proportional to the acceleration of photoexcited carriers, is emitted into free space. Since the effective mass of holes is much larger than that of electrons, holes are considered to be almost localized in each quantum well and, therefore, the emitted THz signal is dominated by the acceleration of electrons in the miniband. The emitted E_{THz} was detected in a reflection geometry by the free-space THz electro-optic (EO) sampling technique.^{26,27} The EO sampling technique has two advantages: First, it measures E_{THz} and is sensitive both to the amplitude and phase of the emitted THz radiation. This is

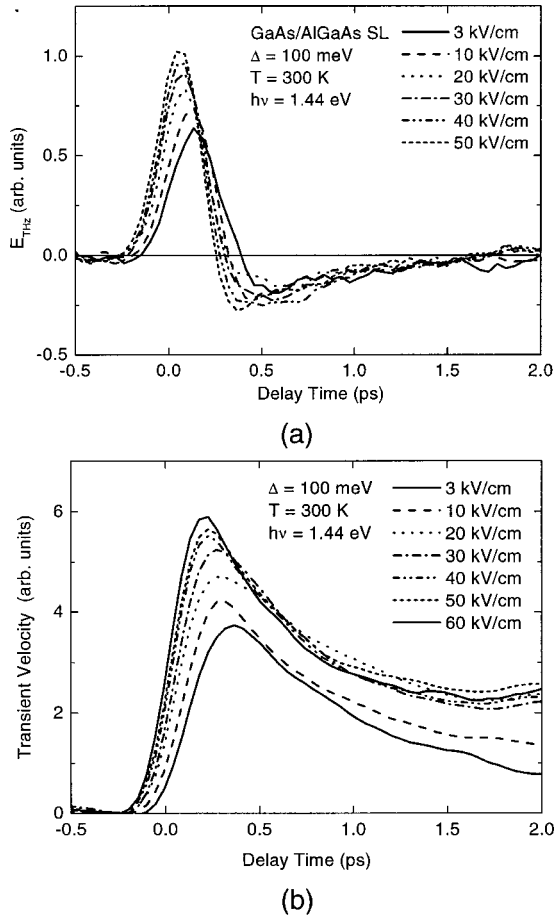


FIG. 1. Detected THz electric field (a) and the transient electron velocity obtained by integrating the THz signal (b) are plotted as a function of delay time when the bottom of the miniband is photoexcited ($\hbar\omega = 1.44$ eV).

advantageous over other detection techniques which measure the power of the emitted radiation.²⁵ Second, since the sample is excited only once by the pump pulse, the information at zero time delay is not lost; in other techniques such as four-wave mixing or transmittive electro-optic sampling, the sample is excited both by the pump and probe pulses and, therefore, the signal at zero time delay is plagued by an instantaneous peak.⁸ The EO sensor used in this experiment was a 100- μm -thick (110) ZnTe crystal, which has a cutoff frequency of about 5 THz (corresponding time resolution ~ 200 fs). The time resolution in this experiment could be improved with the use of thinner EO sensor crystals.²⁸ However, this would also proportionally cut down the signal amplitude. Since the THz signal emitted from SL's is relatively weak due to their transport in a limited miniband width, the use of much thinner detection crystals would pull the signal below the noise floor in our shot-noise-limited detection system, which has a relative sensitivity of about $10^{-8}/\sqrt{\text{Hz}}$. Therefore, a 100- μm -thick ZnTe is a compromise between the detection bandwidth and the sensitivity. All the measurements were carried out at room temperature.

In Fig. 1(a), E_{THz} measured at various applied electric fields F is plotted as a function of the delay time. For this experiment, we set the pump photon energy $\hbar\omega$ in such a

way that the electrons are photoexcited at the bottom of the miniband ($\hbar\omega = 1.44$ eV). It can be seen that, at low-bias electric fields, E_{THz} gradually increases and reaches a peak value about 150 fs after photoexcitation. This is followed by a decrease until it reaches zero acceleration around 400 fs. Here E_{THz} , then, becomes negative, which corresponds to carrier deceleration. With an increase in the bias field, the peak acceleration attained increases and occurs at earlier times. The negative feature is slightly more pronounced for larger bias fields and a shift to earlier times is clearly distinguishable.

The acceleration traces shown in Fig. 1(a) were integrated once with respect to time to obtain the transient velocities and are plotted in Fig. 1(b) for various applied bias fields F . The velocity at $F = 3$ kV/cm increases, reaches a maximum, and slightly decreases before it reaches a steady-state value approximately 2 ps after photoexcitation. As F is increased, the maximum carrier velocity increases and also occurs at earlier times. The time taken for electrons to reach their steady-state velocity is typically around 2 ps, suggesting that the energy relaxation time in the present superlattice is of this order. This is one order of magnitude longer than the energy relaxation times of the order of a few hundred femtoseconds that have been estimated by transport experiments.^{29,30}

In the case of bulk GaAs, the velocity overshoot phenomenon is understood to be due to the intervalley scattering and exhibits well-known transient velocity characteristics.²⁴ In the case of superlattices, however, electrons are accelerated beyond the inflection point of the Brillouin zone before they are scattered to higher valleys. Beyond the inflection point, the effective mass for miniband transport becomes negative. Therefore, when a significant fraction of electrons populate the dispersion beyond the inflection point, the electron drift velocity starts decreasing. We can make a rough estimate of the time taken for the electrons to reach the inflection point, Δt , by solving a simple equation of ballistic motion, $\hbar\Delta k_z = eF\Delta t$, and setting $\Delta k_z = \pi/2d$, where \hbar is the reduced Planck constant and k_z the momentum in the SL direction. Assuming $F = 3$ kV/cm, we find that Δt is about 500 fs, which is in reasonable agreement with the time for the transient velocity to reach its maximum value experimentally observed for $F = 3$ kV/cm. For higher electric fields, Δt becomes much shorter and the signal lies beyond the detection bandwidth of the EO sensor used.

Now let us look at the steady-state velocity of electrons. As is well known, SL's exhibit NDV's beyond a critical bias field.^{1,17-21} In Fig. 2, electron drift velocities determined at 2 ps after photoexcitation from the time-domain data [Fig. 1(b)] are plotted by solid circles as a function of F . It can be seen that for low-bias fields the drift velocity increases before it reaches a constant value beyond 20 kV/cm. The photocurrent through the Schottky diode during the measurements, plotted in the inset in the same figure, is also found to slightly decrease for $F > 20$ kV/cm. These behaviors are reminiscent of the existence of NDV's of electrons beyond a critical field.

In the case of excitation at the bottom of the miniband, carriers are created at states with $k_{xy} \sim k_z \sim 0$, where k_{xy} is

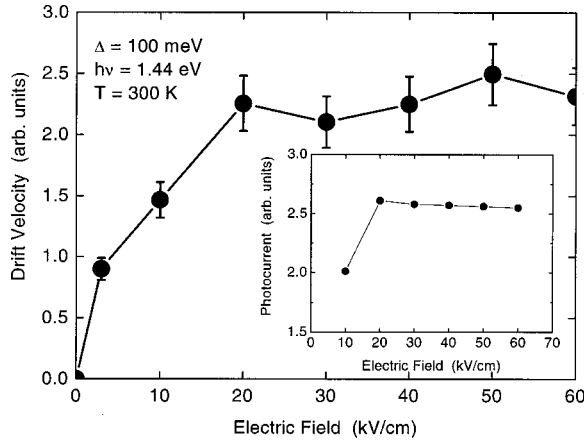
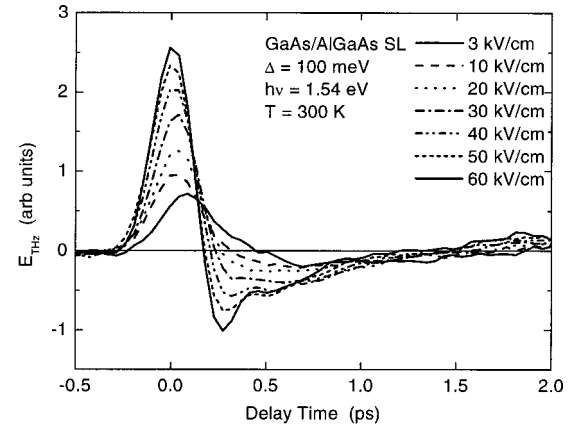


FIG. 2. Steady-state drift velocity as a function of applied bias field for the photoexcitation at the bottom (solid circles) of the miniband. The inset shows the photocurrent across the Schottky diode as a function of the applied bias field during the THz measurements.

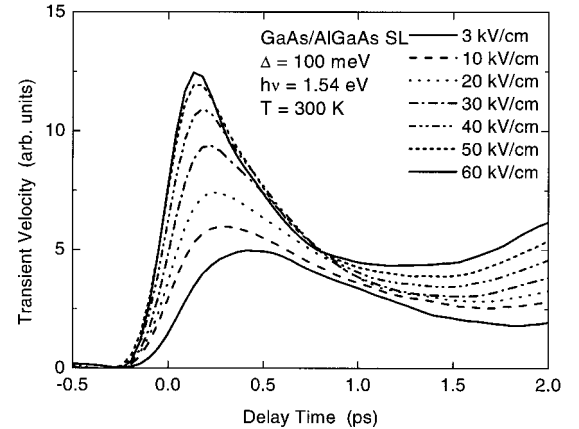
the electron momentum in the in-plane direction. In this case, when the electrons are subjected to instantaneous acceleration in the presence of the applied bias field, they are accelerated almost in phase from $k_z \sim 0$. If, on the other hand, the carriers are excited at the top of the miniband, then, from a simple one-dimensional picture, one would expect that they be Bragg reflected and start moving in a direction opposite to the applied bias field. This would, then, correspond to a phase reversal in E_{THz} . Figures 3(a) and 3(b) show E_{THz} and the transient velocities, respectively, when electrons are excited at the top of the miniband ($\hbar\omega = 1.54$ eV). It is clearly seen that no such phase reversal in E_{THz} is observed. E_{THz} , in fact, exhibits a similar behavior to the case of the excitation at the bottom of the miniband ($\hbar\omega = 1.44$ eV).

When carriers are photoexcited at the top of the miniband ($\hbar\omega = 1.54$ eV), because of the continuous lateral dispersion, not only electrons with $k_z \sim \pi/d$ and $k_{xy} \sim 0$, but also electrons with finite k_{xy} and smaller k_z are created. Therefore, electrons are not accelerated from well-defined initial quantum states and the emitted THz radiation is proportional to an ensemble average of electron acceleration of many different quantum states. Furthermore, from a consideration of the density of states, the number of available states for the photoexcited carriers decreases from $k_z = 0$ to $k_z = \pi/d$ as $\propto [\Delta E - E_z(k_z)]^{1/2}$, where ΔE is the excess kinetic energy of photoexcited electrons and $E_z(k_z)$ the kinetic energy in the z direction. This means that the number of carriers created with small k_z is much larger than that near $k_z = \pi/d$ even when the SL is pumped at the top of the miniband. This explains why the behavior of E_{THz} is qualitatively similar in the two cases.

If we look at the traces in Figs. 1 and 3 more closely, however, there are some noticeable differences: for example, the acceleration and deceleration observed at low F for $\hbar\omega = 1.54$ eV is less steep than for $\hbar\omega = 1.44$ eV. This is due to ensemble averaging effect of THz radiation generated by electrons with different initial quantum states; since the pho-



(a)



(b)

FIG. 3. Detected THz electric field (a) and the transient electron velocity obtained by integrating the THz signal (b) are plotted as a function of delay time when the top of the miniband is photoexcited ($\hbar\omega = 1.54$ eV).

toexcited electrons with initial $k_z > \pi/2d$ are accelerated in the direction opposite to F , they partly cancel the acceleration THz signal due to the majority electrons with initial $k_z < \pi/2d$.

In conclusion, the bias and excitation energy dependence of the nonequilibrium transport properties of electrons in a wide miniband GaAs/Al_{0.3}Ga_{0.7}As superlattice is presented. The transient electron velocity shows acceleration-deceleration features that are characteristic of the miniband dispersion. Electron velocity is found to reach its steady-state value approximately ~ 2 ps after the excitation, suggesting that the energy relaxation times in these structures is of this order. When pumped at the top of the miniband, no phase reversal in the transient velocity was observed, owing to a large density of quantum states near $k_z \sim 0$.

The authors thank A. Leitenstorfer for valuable discussions. This work was supported by CREST of the Japan Science and Technology Corporation, a Grant-in-Aid from Japan Society for the Promotion of Science (No. 12450140), a Grant-in-Aid for COE research from MEXT (No. 12CE2004), and NEDO international collaboration program.

* Also with CREST, Japan Science and Technology Corporation.

† Electronic address: hirakawa@nano.iis.u-tokyo.ac.jp

- ¹L. Esaki and R. Tsu, *IBM J. Res. Dev.* **14**, 61 (1970).
- ²J. Bleuse, G. Bastard, and P. Voisin, *Phys. Rev. Lett.* **60**, 220 (1988).
- ³E. E. Mendez, F. Agulló-Rueda, and J. M. Hong, *Phys. Rev. Lett.* **60**, 2426 (1988).
- ⁴P. Voisin, J. Bleuse, C. Bouche, S. Gaillard, C. Alibert, and A. Regreny, *Phys. Rev. Lett.* **61**, 1639 (1988).
- ⁵K. Leo, P. H. Bolivar, F. Brüggermann, R. Schwedler, and K. Köhler, *Solid State Commun.* **84**, 943 (1992).
- ⁶J. Feldmann, K. Leo, J. Shah, D. A. B. Miller, J. E. Cunningham, T. Meier, G. Von Plessan, A. Shulze, P. Thomas, and S. Schmitt-Rink, *Phys. Rev. B* **46**, 7252 (1992).
- ⁷C. Waschke, H. G. Roskos, R. Schwedler, K. Leo, H. Kurz, and K. Köhler, *Phys. Rev. Lett.* **70**, 3319 (1993).
- ⁸T. Dekorsy, P. Leisching, K. Köhler, and H. Kurz, *Phys. Rev. B* **50**, R8106 (1994).
- ⁹P. Leishing, P. H. Bolivar, R. Schwedler, K. Leo, H. Kurz, K. Köhler, and P. Ganser, *Semicond. Sci. Technol.* **9**, 419 (1994).
- ¹⁰T. Dekorsy, R. Ott, H. Kurz, and K. Köhler, *Phys. Rev. B* **51**, 17 275 (1995).
- ¹¹G. C. Cho, T. Dekorsy, H. J. Bakker, H. Kurz, A. Kohl, and B. Opitz, *Phys. Rev. B* **54**, 4420 (1996).
- ¹²V. G. Lyssenko, G. Valušis, F. Loser, T. Hasche, K. Leo, M. M. Dignam, and K. Kohler, *Phys. Rev. Lett.* **79**, 301 (1997).
- ¹³K. Leo, *Semicond. Sci. Technol.* **13**, 249 (1998) (topical review).
- ¹⁴M. Sudzius, V. G. Lyssenko, F. Löser, K. Leo, M. M. Dignam, and K. Köhler, *Phys. Rev. B* **57**, R12 693 (1998).
- ¹⁵M. Först, G. Segschneider, T. Dekorsy, H. Kurz, and K. Köhler, *Phys. Rev. B* **61**, R10 563 (2000).
- ¹⁶T. Dekorsy, A. Bartels, H. Kurz, K. Köhler, R. Hey, and K. Ploog, *Phys. Rev. Lett.* **85**, 1080 (2000).
- ¹⁷A. Sibille, J. F. Palmier, H. Wang, and F. Mollot, *Phys. Rev. Lett.* **64**, 52 (1990).
- ¹⁸A. Sibille, J. F. Palmier, H. Wang, J. C. Esnault, and F. Mollot, *Appl. Phys. Lett.* **56**, 256 (1990).
- ¹⁹A. Sibille, J. F. Palmier, C. Minot, and F. Mollot, *Appl. Phys. Lett.* **54**, 165 (1989).
- ²⁰H. T. Grahn, K. Von Klitzing, K. Ploog, and G. H. Dohler, *Phys. Rev. B* **43**, 12 094 (1991).
- ²¹S. Khorram, J. Jo, K. L. Wang, T. Block, and D. Streit, *Phys. Rev. B* **51**, 17 614 (1995).
- ²²E. Schomburg, M. Henini, J. M. Chamberlain, D. P. Steenson, S. Brandl, K. Hofbeck, K. F. Renk, and W. Wegscheider, *Appl. Phys. Lett.* **74**, 2179 (1999).
- ²³E. Schomburg, T. Blomeier, K. Hofbeck, J. Grenzer, S. Brandl, I. Lingott, A. A. Ignatov, K. F. Renk, D. G. Pavel'ev, Yu. Koschurinov, B. Ya. Melzer, V. M. Ustinov, S. V. Ivanov, A. Zhukov, and P. S. Kop'ev, *Phys. Rev. B* **58**, 4035 (1998).
- ²⁴A. Leitenstorfer, S. Hunsche, J. Shah, M. C. Nuss, and W. H. Knox, *Phys. Rev. Lett.* **82**, 5140 (1999).
- ²⁵Y. Shimada, T. Matsuno, and K. Hirakawa, *Jpn. J. Appl. Phys., Part 1* **40**, 3009 (2001).
- ²⁶A. Leitenstorfer, S. Hunsche, J. Shah, M. C. Nuss, and W. H. Knox, *Appl. Phys. Lett.* **74**, 1516 (1999).
- ²⁷Q. Wu and X.-C. Zhang, *Appl. Phys. Lett.* **71**, 1285 (1997).
- ²⁸Q. Wu and X.-C. Zhang, *IEEE J. Quantum Electron.* **2**, 693 (1996).
- ²⁹C. Minot, H. Le Person, J. F. Palmier, and F. Mollot, *Phys. Rev. B* **47**, 10 024 (1993).
- ³⁰S. Winnerl, E. Schomburg, J. Grenzer, H.-J. Regl, A. A. Ignatov, A. D. Semenov, K. F. Renk, D. G. Pavel'ev, Yu. Koschurinov, B. Melzer, V. Ustinov, S. Ivanov, S. Schaposchnikov, and P. S. Kop'ev, *Phys. Rev. B* **56**, R10 303 (1997).